

Research



Cite this article: Zohdi T.I. 2016 On firework blasts and qualitative parameter dependency. *Proc. R. Soc. A* **472**: 20150720.
<http://dx.doi.org/10.1098/rspa.2015.0720>

Received: 17 October 2015

Accepted: 9 December 2015

Subject Areas:

mechanical engineering

Keywords:

fireworks, blast radius, simulation

Author for correspondence:

T. I. Zohdi

e-mail: zohdi@berkeley.edu

On firework blasts and qualitative parameter dependency

T. I. Zohdi

Department of Mechanical Engineering, 6195 Etchevery Hall,
University of California, Berkeley, CA 94720-1740, USA

In this paper, a mathematical model is developed to qualitatively simulate the progressive time-evolution of a blast from a simple firework. Estimates are made for the blast radius that one can expect for a given amount of detonation energy and pyrotechnic display material. The model balances the released energy from the initial blast pulse with the subsequent kinetic energy and then computes the trajectory of the material under the influence of the drag from the surrounding air, gravity and possible buoyancy. Under certain simplifying assumptions, the model can be solved for analytically. The solution serves as a guide to identifying key parameters that control the evolving blast envelope. Three-dimensional examples are given.

1. Introduction

Fireworks are widely used in cultural celebrations, sporting events, political rallies, etc. The full sequence of events for release of a cloud of packed material begins with an initiated detonation that rapidly rips open a thin container (typically a lightweight shell of cardboard), which releases packed pyrotechnic powder particles forming a cloud. Various compounds are mixed together to produce a wide array of colours (e.g. blue (caesium, copper), red (lithium), orange (calcium), yellow (iron), etc.). For a history of fireworks, we refer the interested reader to Plimpton [1], Brock [2], Russell [3], Shimanzu [4], Werrett [5] and Kazuma [6,7].

In this paper, we are primarily interested in qualitatively estimating the time-evolution of the envelope of a cloud emanating from a firework blast (figure 1). The estimation of the time-evolution and the size of the blast is important for both aesthetic and safety reasons. Thus, the main objective of this study is to



Figure 1. Time-lapse photo of firework material emanating from a blast. Photo available courtesy of the public domain site <http://www.photos-public-domain.com/wp-content/uploads/2011/07/>. (Online version in colour.)

develop a practical qualitative model which captures the essential physics of detonation and blast envelope growth. A schematic of the model problem is shown in figure 2. In this work, we do not consider detailed models for the interaction between the shock wave and the packed particles (e.g. [8–11]) nor the chemical aspects which are beyond the scope of this work.¹ We make the following simplifying assumptions:

- The fragments do not interact with one another.
- The blast fragments are all the same size, assumed spherical with radius $R_i = R$ and receive the same velocity pulse (denoted $\delta v(0)$), in the radial direction from the centre of the blast upon detonation. Specifically, the velocity vector pulse is radially outward from the centre of the sphere, co-located at the centre of mass of the pyrotechnic display material

$$\delta v_i(0) = \|\delta v(0)\| \left(\frac{\mathbf{r}_i(0) - \mathbf{r}_c(0)}{\|\mathbf{r}_i(0) - \mathbf{r}_c(0)\|} \right) \stackrel{\text{def}}{=} \|\delta v(0)\| \mathbf{n}_{ri}, \quad (1.1)$$

where \mathbf{r}_i is the position vector of the i th particle, \mathbf{n}_{ri} is the normal/radial direction and

$$\mathbf{r}_c(0) = \frac{1}{\left(\sum_{i=1}^N m_i\right)} \sum_{i=1}^N m_i \mathbf{r}_i(0), \quad (1.2)$$

where N is the number of particles, $\mathbf{r}_c(0)$ is the centre of mass of the packed particles and m_i is the mass of each particle. The pulse velocities are added to the velocity vectors immediately before the pulse ($v^-(0)$)

$$\mathbf{v}_i^+(0) = \mathbf{v}_i^-(0) + \delta v_i(0). \quad (1.3)$$

¹See Martin-Alberca & Garcia-Ruiz [12] for an overview of common consumer fireworks, their usual chemical compositions, and some important classification and legal regulations in Western countries.

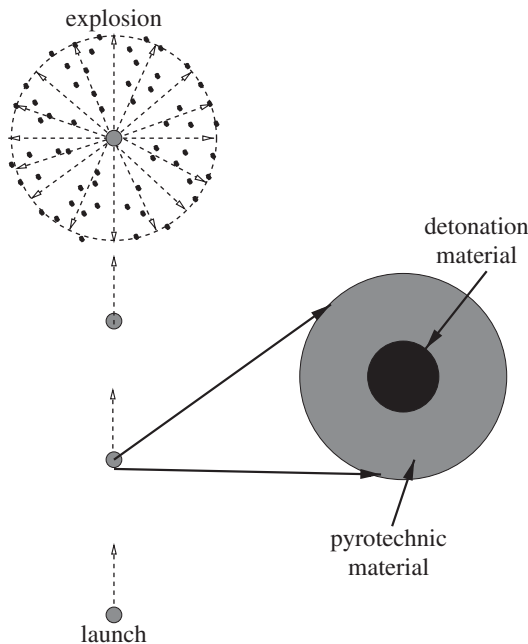


Figure 2. Launch and detonation of a firework.

- The magnitude of the initial velocity pulse dictates initial energy released (E), which is assumed to be converted into kinetic energy for the pyrotechnic material at ($t = 0$)

$$E = \sum_{i=1}^N \frac{1}{2} m_i \|\delta v(0)\|^2 \Rightarrow \|\delta v(0)\| = \sqrt{\frac{2E}{\sum_{i=1}^N m_i}} = \sqrt{\frac{2E}{M}}, \quad (1.4)$$

where $\delta v(0)$ is the velocity of pulse imparted to a fragment in the radial direction, M is the total pyrotechnic material mass, $m_i = \rho_i \frac{4}{3} \pi R_i^3$ is mass of the individual fragments, where ρ_i is the density of the fragments.

- The objects in the system are assumed to be small enough to be considered (idealized) as particles, spherical in shape, and that the effects of their rotation with respect to their mass centre are unimportant to their overall motion. The equation of motion for the i th particle in the system is (with $m_i = m$)

$$m \dot{\mathbf{v}}_i = \boldsymbol{\Psi}_i^{\text{tot}} = \boldsymbol{\Psi}_i^{\text{drag}} + \boldsymbol{\Psi}_i^{\text{grav}} + \boldsymbol{\Psi}_i^{\text{buoy}}, \quad (1.5)$$

with initial velocity $\mathbf{v}_i(0)$ and initial position $\mathbf{r}_i(0)$. The gravitational force is $\boldsymbol{\Psi}_i^{\text{grav}} = m\mathbf{g}$, where $\mathbf{g} = (g_x, g_y, g_z) = (0, 0, -9.81) \text{ m s}^{-2}$. The buoyancy force is $\boldsymbol{\Psi}_i^{\text{buoy}} = \rho_a \frac{4}{3} \pi R^3 \mathbf{b} \stackrel{\text{def}}{=} m_a \mathbf{b}$, where $\mathbf{b} = (b_x, b_y, b_z) = (0, 0, 9.81) \text{ m s}^{-2}$ and ρ_a is the density of air. Buoyancy can be important because of the potentially porous nature of the fragments.

- For the drag, we will employ a general phenomenological model

$$\boldsymbol{\Psi}_i^{\text{drag}} = \frac{1}{2} \rho_a C_D \|\mathbf{v}^f - \mathbf{v}_i\| (\mathbf{v}^f - \mathbf{v}_i) A, \quad (1.6)$$

where C_D is the drag coefficient, A is the reference area, which for a sphere is $A = \pi R^2$, ρ_a is the density of the ambient fluid environment and \mathbf{v}^f is the velocity of the surrounding medium which, in the case of interest, is air.

Remark 1.1. Later, we will assume that $\mathbf{v}^f \approx 0$, implicitly assuming that the dynamics of the surrounding medium is unimportant. However, for other applications, such as high-speed flow,

the motion of the surrounding fluid can be important, necessitating fully coupled (two-way) particle–fluid interaction models. This is outside the scope of the present work. Generally, this requires the use of solid–fluid staggering-type schemes (e.g. [13–19]). This is discussed further at the end of this paper.

Remark 1.2. For the problems under consideration, the non-interaction assumption is quite appropriate since all of the particles are propagating radially outwards with the same initial velocity. Thus, their mutual collisions are negligible. This was also checked against ‘brute-force’ simulations, which are beyond the scope of this paper, using formulations in Zohdi [16,17] which take detailed collisions into account.

2. General fragment trajectories

The differential equation for each fragment in its outward normal direction is ($m_i = m$), assuming no gravity, buoyancy or fluid velocity ($\mathbf{v}^f = \mathbf{0}$). The subscript n indicates the outward normal direction

$$m\dot{v}_{\text{in}} = -\frac{1}{2}\rho_a C_D v_{\text{in}}^2 A, \quad (2.1)$$

where v_{in} is the outward normal velocity, which can be written as

$$\dot{v}_{\text{in}} = -K v_{\text{in}}^2, \quad (2.2)$$

where for a sphere

$$K = \frac{1}{2m} C_D \rho_a A = \frac{3C_D \rho_a}{8\rho R}. \quad (2.3)$$

Using the chain rule

$$\frac{dv_{\text{in}}}{dt} = \frac{dv_{\text{in}}}{dr_{\text{in}}} \frac{dr_{\text{in}}}{dt} = \frac{dv_{\text{in}}}{dr_{\text{in}}} v_{\text{in}} = -K v_{\text{in}}^2, \quad (2.4)$$

which yields

$$\frac{dv_{\text{in}}}{dr_{\text{in}}} = -K v_{\text{in}}, \quad (2.5)$$

and subsequently

$$\frac{dv_{\text{in}}}{v_{\text{in}}} = -K dr_{\text{in}} \Rightarrow \int_{v_{\text{oin}}}^{v_{\text{in}}(t)} \frac{dv_{\text{in}}}{v_{\text{in}}} = - \int_{r_{\text{oin}}}^{r_{\text{in}}(t)} K dr_{\text{in}}, \quad (2.6)$$

where r_{in} is the outward normal position, with solution

$$v_{\text{in}}(t) = v_{\text{oin}} e^{-K(r_{\text{in}}(t) - r_{\text{oin}})}, \quad (2.7)$$

with inverse solution, for the blast radius

$$\mathcal{L}(t) = r_{\text{in}}(t) - r_{\text{oin}} = -\frac{1}{K} \text{Ln} \left(\frac{v_{\text{in}}(t)}{v_{\text{oin}}} \right) = -\frac{8\rho R}{3C_D \rho_a} \text{Ln} \left(\frac{v_{\text{in}}(t)}{v_{\text{oin}}} \right), \quad (2.8)$$

where $1/K$ has units of metres. This shows the explicit inverse relationship between the size of the blast radius and K , which is a measure of the drag (tending to limit the blast radius growth) and the mass (tending to increase the blast radius growth). One can relate this directly to the energy of detonation and total mass via equation (1.4), using $v_{\text{oin}} = \sqrt{2E/M}$

$$\mathcal{L}(t) = r_{\text{in}}(t) - r_{\text{oin}} = -\frac{8\rho R}{3C_D \rho_a} \text{Ln} \left(\frac{v_{\text{in}}(t)}{\sqrt{2E/M}} \right). \quad (2.9)$$

Remark. One could directly integrate equation (2.2) in time to yield

$$v_{\text{in}}(t) = \frac{v_{\text{oin}}}{Kt v_{\text{oin}} + 1} = \frac{\sqrt{2E/M}}{Kt\sqrt{2E/M} + 1} \quad (2.10)$$

and

$$r_{\text{in}}(t) = r_{\text{oin}} + \frac{1}{K} \text{Ln}(Kt v_{\text{oin}} + 1) = r_{\text{oin}} + \frac{1}{K} \text{Ln} \left(Kt \sqrt{\frac{2E}{M}} + 1 \right). \quad (2.11)$$

One can also invert equation (2.11) to yield an expression for the time it takes to achieve a certain blast radius

$$t = \frac{e^{K(r_{\text{in}}(t) - r_{\text{oin}})} - 1}{K\sqrt{2E/M}}. \quad (2.12)$$

3. Hybrid drag

Generally speaking, the drag coefficient, which is an empirical parameter which attempts to represent the action of the fluid forces on an object, is not a constant, and would vary with, for example, the Reynolds number. In the zero Reynolds number limit the drag would be that of a Stokesian regime. One possible way to represent the drag coefficient is with a piecewise definition, as a function of the Reynolds number (Chow [20]):

- for $0 < Re \leq 1$, $C_D = 24/Re$,
- for $1 < Re \leq 400$, $C_D = 24/Re^{0.646}$,
- for $400 < Re \leq 3 \times 10^5$, $C_D = 0.5$,
- for $3 \times 10^5 < Re \leq 2 \times 10^6$, $C_D = 0.000366 Re^{0.4275}$,
- for $2 \times 10^6 < Re < \infty$, $C_D = 0.18$,

where the local Reynolds number for a particle is $Re \stackrel{\text{def}}{=} 2R\rho_a \|v^f - v_i\|/\mu_f$ and μ_f is the fluid viscosity. The viscosity coefficient for air is $\mu_f = 0.000018 \text{ Pa s}^{-1}$. Using the hybrid model reduces the drag at the lower Reynolds number regimes, thus producing a larger blast radius than a constant large drag coefficient. However, to solve the governing equation, when include gravity and buoyancy are included

$$m\dot{v}_i = \Psi_i^{\text{drag}} + \Psi_i^{\text{grav}} + \Psi_i^{\text{buoy}} = \frac{1}{2}\rho_a C_D \|v^f - v_i\| (v^f - v_i) A + mg + mb, \quad (3.1)$$

we integrate the governing equations numerically

$$\begin{aligned} v_i(t + \Delta t) &= v_i(t) + \frac{1}{m} \int_t^{t+\Delta t} (\Psi_i^{\text{drag}} + \Psi_i^{\text{grav}} + \Psi_i^{\text{buoy}}) dt \\ &\approx v_i(t) + \frac{\Delta t}{m} (\Psi_i^{\text{drag}}(t) + \Psi_i^{\text{grav}}(t) + \Psi_i^{\text{buoy}}(t)). \end{aligned} \quad (3.2)$$

Remark. The piecewise drag law of Chow [20] is a mathematical description for the Reynolds number over a wide range and is a curve-fit of extensive data from Schlichting [21]. As observed in the experimental data, the mathematical function exhibits a discontinuity at $Re = 3 \times 10^5$, although in an explosion the time a particle spends at this Reynolds number is almost negligible.

4. Numerical example

In order to illustrate the model, the following simulation parameters were chosen (they are not intended to simulate a specific firework event):

- total simulation duration, 35 s,
- time to detonation after launch, 3 s,
- the time-step size, $\Delta t = 10^{-4}$ s,
- launch velocity, $v(t=0) = (0, 0, 100) \text{ m s}^{-1}$ (starting from a launch height of 1 m),

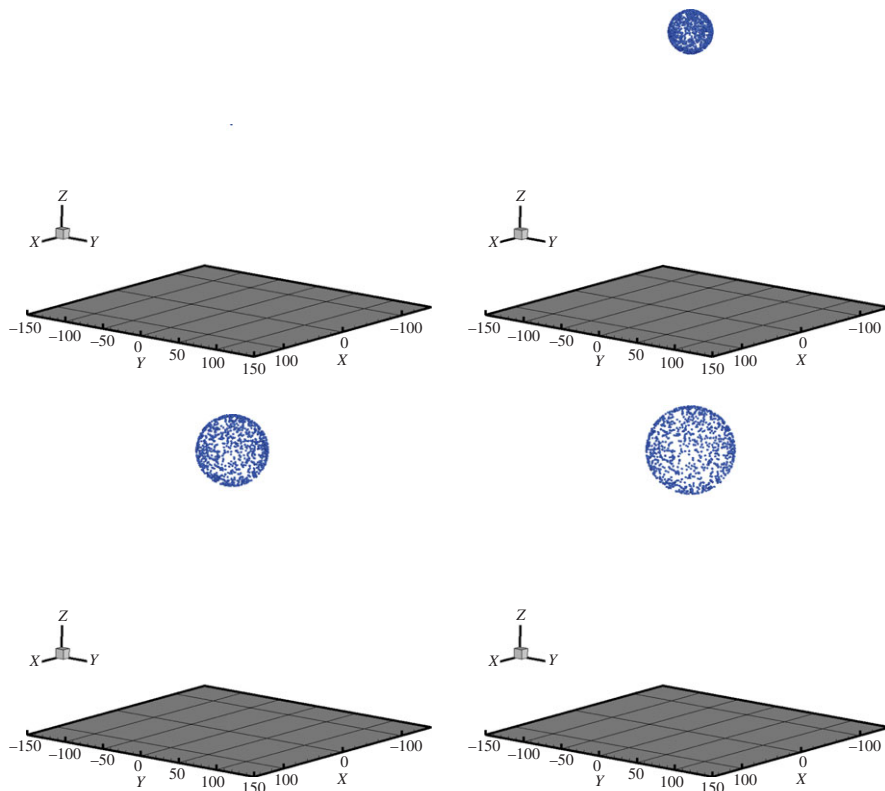


Figure 3. From left to right and top to bottom: initial launch of packed particles (small barely visible point), and then the progressive blast with fragments reaching a maximum height. (Online version in colour.)

- detonation energy, $E = 100\,000\text{ J}$,
- density of air, $\rho_a = 1.225\text{ kg m}^{-3}$,
- core inner packing shell radius (figure 2), $R_o = 0.01\text{ m}$ (which holds the packed detonation material),
- core outer packing shell radius (figure 2), $R_o = 0.025\text{ m}$ (forming a shell of packed pyrotechnic display material),
- number of fragments, $N = 1000$,
- density of pyrotechnic display material, $\rho = 1000\text{ kg m}^{-3}$,
- total mass, $M = \sum_{i=1}^N m_i = 0.5\text{ kg}$,
- the fragment sizes were calculated by $R_i = (M/N\rho\pi(4/3))^{1/3}$ and were packed between the inner and outer shell cited above.

An extremely small (relative to the total simulation time) time-step size of $\Delta t = 10^{-4}\text{ s}$ was used. Further reductions of the time-step size produced no notable changes in the results, thus the solutions generated can be considered to have negligible numerical error. The simulations took under 1 min on a standard laptop. Figures 3 and 4 illustrate the results for the parameters above. With the chosen parameters, the blast radius was approximately 110 m. We note that in the descending phase of the trajectory, the particles nearly achieve a so-called settling steady-state velocity, v_{tm} (when $\dot{v} = 0$), given by assuming a purely vertical trajectory drop

$$\begin{aligned}
 m\dot{v} &= mg + m_a\mathbf{b} + \frac{1}{2}\rho_a A C_D v \|\mathbf{v}\| \Rightarrow 0 \\
 &= -mg + m_a g + \frac{1}{2}\rho_a A C_D v_{tm}^2 \Rightarrow v_{tm} = \sqrt{\frac{2(m - m_a)g}{\rho_a C_D A}},
 \end{aligned}
 \tag{4.1}$$

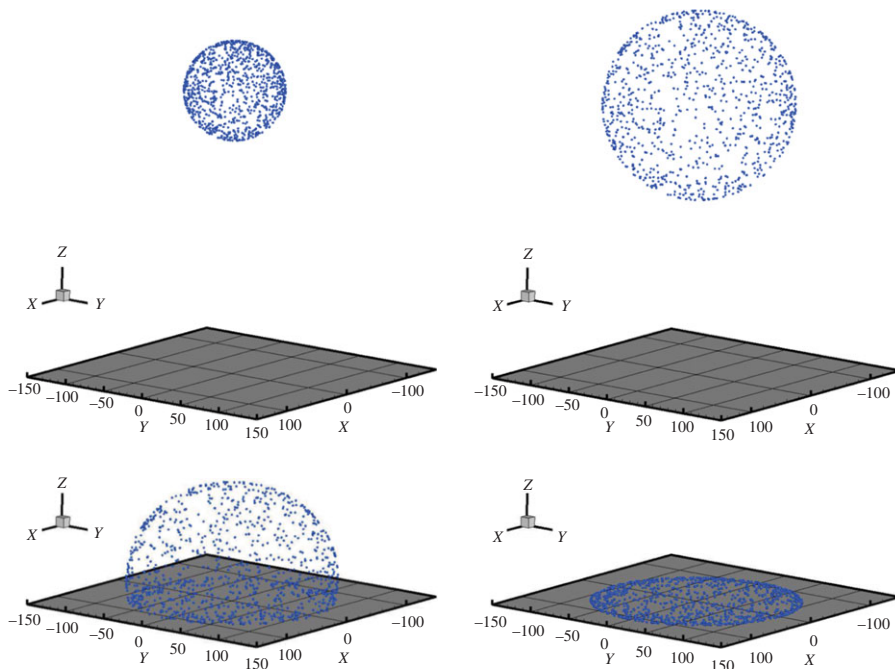


Figure 4. From left to right and top to bottom: descent and settling of the fragments. (Online version in colour.)

where an implicit equation for the settling velocity arises due to the drag coefficient's dependency on $C_D(v)$. We note that the objective of this simulation was not to simulate any specific firework configuration or material, but to illustrate the character of the model. For example, for the pyrotechnic material, the density was selected simply to illustrate the model. When the blast material is ejected, it can be quite porous, not entirely a solid. Thus using a solid density of say, copper or iron, would be inappropriate. Thus, without further information, selecting a density of 1000 kg m^{-3} was a neutral option. This can easily be modified for specific cases.

Remark. In the low velocity (low Reynolds number) limit, a Stokesian model is most appropriate, which is what the hybrid drag law attempts to incorporate. The drag forces are significantly smaller with a Stokesian model. Comparing a purely Stokesian drag law, which would be valid for small particles and laminar flow (low Reynolds number)

$$\psi_i^{\text{drag,Stokesian}} = c(v^f - v_i) = \mu_f 6\pi R_i (v^f - v_i), \quad (4.2)$$

where μ_f is the fluid viscosity. We observe the following:

$$\frac{\|\psi^{\text{drag,Stokesian}}\|}{\|\psi^{\text{drag}}\|} = \frac{12\mu_f}{\rho_a C_D R \|v^f - v_i\|}. \quad (4.3)$$

For typical parameters for air and spherical particles (using $C_D = 0.5$, which is a mid-range value from the piecewise drag law introduced earlier), we have

$$\frac{\|\psi^{\text{drag,Stokesian}}\|}{\|\psi^{\text{drag}}\|} = \frac{12\mu_f}{\rho_a C_D R \|v^f - v_i\|} \approx \frac{0.0004}{R \|v^f - v_i\|}, \quad (4.4)$$

which indicates that for extremely small fragments and low velocities, the Stokesian model dominates, while for larger fragments and large velocities, the phenomenological model dominates. The limiting Stokesian case is discussed further in the appendix.

5. Summary

For general blast conditions, there can be cases where the change in the surrounding fluid's behaviour due to the motion of the particles may be important. With those cases in mind, had the fragment non-interaction approximation not been invoked, a coupled system of equations would arise due to the interaction between the fragments. For example, this entails numerically integrating, in an implicit manner, the governing equations, which leads to (for example using a trapezoidal rule with variable integration metric, $0 \leq \phi \leq 1$)

$$\begin{aligned} v_i(t + \Delta t) &= v_i(t) + \frac{1}{m} \int_t^{t+\Delta t} (\Psi_i^{\text{grav}} + \sum_{j=1, j \neq i}^K \Psi_{ij} + \Psi_i^{\text{fluid}}) dt \\ &\approx v_i(t) + \frac{\Delta t \phi}{m} \left(\Psi_i^{\text{grav}}(t + \Delta t) + \sum_{j=1, j \neq i}^K \Psi_{ij}(t + \Delta t) + \Psi_i^{\text{fluid}}(t + \Delta t) \right) \\ &\quad + \frac{\Delta t(1 - \phi)}{m} \left(\Psi_i^{\text{grav}}(t) + \sum_{j=1, j \neq i}^K \Psi_{ij}(t) + \Psi_i^{\text{fluid}}(t) \right), \end{aligned} \quad (5.1)$$

where Ψ_i^{fluid} represents the interaction of fragment i with the fluid and $\Psi_{ij}(t)$ represents its interaction with the neighbouring $j = 1, 2, \dots, K$ fragments. The position can be computed via application of the trapezoidal rule again:

$$r_i(t + \Delta t) \approx r_i(t) + \Delta t(\phi v_i(t + \Delta t) + (1 - \phi)v_i(t)), \quad (5.2)$$

which can be consolidated into

$$\begin{aligned} r_i(t + \Delta t) &= r_i(t) + v_i(t)\Delta t \\ &\quad + \frac{\phi^2(\Delta t)^2}{m} \left(\Psi_i^{\text{grav}}(t + \Delta t) + \sum_{j=1, j \neq i}^K \Psi_{ij}(t + \Delta t) + \Psi_i^{\text{fluid}}(t + \Delta t) \right) \\ &\quad + \frac{\phi(1 - \phi)(\Delta t)^2}{m} \left(\Psi_i^{\text{grav}}(t) + \sum_{j=1, j \neq i}^K \Psi_{ij}(t) + \Psi_i^{\text{fluid}}(t) \right). \end{aligned} \quad (5.3)$$

This yields a coupled system of equations for the interaction between the fragments and the fluid, which would necessitate spatio-temporal discretization for example using finite-element, finite difference, finite volume or discrete element methods, such as those found in Onate *et al.* [22,23,25], Avci & Wriggers [19], Leonardi *et al.* [24], Bolintineanu *et al.* [26] and Zohdi [13–18]. Furthermore, in order to obtain more accurate initial conditions for the system, advanced models would also involve detailed modelling of the initial packing of the material [27,28], and the evolution of heat and the mechanics of the surrounding fluid environment. Such systems are quite complex. Thus, in order to qualitatively understand such systems *a priori*, the results presented in this paper are useful. Summarizing, in the absence or gravity of buoyancy, one obtains quite simple relations for the velocity of the fragments (under the constant drag coefficient assumption)

$$v_{\text{in}}(t) = v_{\text{oin}} e^{-K(r_{\text{in}}(t) - r_{\text{oin}})} = \sqrt{\frac{2E}{M}} e^{-(3C_D \rho_a / 8\rho R)(r_{\text{in}}(t) - r_{\text{oin}})}, \quad (5.4)$$

with inverse solution, for the blast radius

$$\mathcal{L}(t) = r_{\text{in}}(t) - r_{\text{oin}} = -\frac{8\rho R}{3C_D \rho_a} \text{Ln} \left(\frac{v_{\text{in}}}{v_{\text{oin}}} \right) = -\frac{8\rho R}{3C_D \rho_a} \text{Ln} \left(\frac{v_{\text{in}}}{\sqrt{2E/M}} \right). \quad (5.5)$$

Under the non-interaction approximation made earlier, the expressions above can be used for each fragment to compute the trajectory and provide a useful guide for more detailed studies, which are being currently pursued by the author.

Competing interests. There are no competing interests.

Funding. This work was funded in part by the Army Research Laboratory through the Army High Performance Computing Research Center (cooperative agreement number W911NF-07-2-0027).

Appendix A. Stokesian model

The differential equation for each fragment is ($m_i = m$)

$$m \frac{d\mathbf{v}_i}{dt} = c(\mathbf{v}^f - \mathbf{v}_i) + m\mathbf{g} + m_a \mathbf{b} \quad (\text{A } 1)$$

and can be solved analytically in the normal direction (\mathbf{n}_{ri}) to yield

$$v_{in}(t) = \left(v_{in}(0) - v_n^f - \frac{m}{c} \left(g_n + \frac{m_a}{m} b_n \right) \right) e^{-(c/m)t} + v_n^f + \frac{m}{c} \left(g_n + \frac{m_a}{m} b_n \right). \quad (\text{A } 2)$$

The position in the normal direction is

$$r_{in}(t) = r_{in}(0) + A_{in} \frac{m}{c} (1 - e^{-(c/m)t}) + B_{in} t, \quad (\text{A } 3)$$

where $A_{in} = v_{in}(0) - v_n^f - (m/c)(g_n + (m_a/m)b_n)$ and $B_{in} = v_n^f + (m/c)(g_n + (m_a/m)b_n)$. We note that

$$\frac{m}{c} = \frac{2R^2 \rho}{9\mu_f}. \quad (\text{A } 4)$$

(a) Gravity and buoyancy-free case

In the normal direction, with no gravity and buoyancy, this collapses to a particularly simple expression for the velocity of each fragment

$$v_{in}(t) = v_{in}(0) e^{-(c/m)t} \quad (\text{A } 5)$$

and for the position, we have

$$r_{in}(t) = r_{in}(0) + v_{in}(0) \frac{m}{c} (1 - e^{-(c/m)t}). \quad (\text{A } 6)$$

(b) Blast envelope radius

To extract the 'pure' blast envelope radius, ignoring the launch velocity, thus $v_{in}(0) = \|\delta\mathbf{v}(0)\|$

$$v_{in}(t) = v_{in}(0) e^{-(c/m)t} = \|\delta\mathbf{v}_{in}(0)\| e^{-(c/m)t} \quad (\text{A } 7)$$

and for the position, we have

$$r_{in}(t) = r_{in}(0) + v_{in}(0) \frac{m}{c} (1 - e^{-(c/m)t}) = r_{in}(0) + \|\delta\mathbf{v}_{in}(0)\| \frac{m}{c} (1 - e^{-(c/m)t}). \quad (\text{A } 8)$$

Using equation (1.4) yields

$$v_{in}(t) = \left(\sqrt{\frac{2E}{M}} \right) e^{-(9\mu_f/2R^2\rho)t} \quad (\text{A } 9)$$

and

$$r_{in}(t) = r_{in}(0) + \left(\sqrt{\frac{2E}{M}} \frac{2\rho R^2}{9\mu_f} \right) (1 - e^{-(9\mu_f/2R^2\rho)t}). \quad (\text{A } 10)$$

We define the blast radius

$$\mathcal{L}(t) \stackrel{\text{def}}{=} r_{in}(t) - r_{in}(0) = \left(\sqrt{\frac{2E}{M}} \frac{2\rho R^2}{9\mu_f} \right) (1 - e^{-(9\mu_f/2R^2\rho)t}). \quad (\text{A } 11)$$

The maximum radius ($t = \infty$) is

$$\mathcal{L}(t = \infty) = \left(\sqrt{\frac{2E}{M}} \frac{2\rho R^2}{9\mu_f} \right). \quad (\text{A } 12)$$

The ratio of the radius at any given time to the maximum is

$$\frac{\mathcal{L}(t)}{\mathcal{L}_\infty} = 1 - e^{-(9\mu_f/2R^2\rho)t}. \quad (\text{A } 13)$$

To determine the time for the blast radius to achieve a certain size, $\mathcal{L}(t^*) = \mathcal{L}^*$, we may solve for the time from the above

$$t^* = -\frac{2\rho R^2}{9\mu_f} \text{Ln} \left(\frac{\mathcal{L}(\infty) - \mathcal{L}^*}{\mathcal{L}(\infty)} \right). \quad (\text{A } 14)$$

The key observations are the exponential (decay-type) growth of the cloud, controlled by the amount of energy in the detonation and the ratio of the surrounding damping and the fragment masses. The growth of the blast sphere is exponential and is controlled by the ratio of the inertial and drag forces, $2R^2\rho/9\mu_f$. The size of the blast sphere is proportional to the square of the size of the particles, the square root of the stored detonation energy, inversely proportional to the square-root of the mass and inversely proportional to the viscosity of the atmosphere. As for the model used in the body of the paper, we note that in the descending phase of the trajectory, for a Stokesian regime, the particles nearly achieve a so-called settling steady-state velocity, v_{tm} (when $\dot{v} = 0$), given by assuming a purely vertical trajectory drop

$$\begin{aligned} m\dot{v} &= mg + m_a b + \mu_f 6\pi R^2 v \Rightarrow 0 \\ &= -mg + m_a g + \mu_f 6\pi R^2 v_{tm} \Rightarrow v_{tm} = \frac{2(\rho - \rho_a)}{9\mu_f} g R^2. \end{aligned} \quad (\text{A } 15)$$

References

1. Plimpton G. 1984 *Fireworks: a history and celebration*. New York, NY: Doubleday.
2. St. Hill Brock A. 1949 *A history of fireworks*. London, UK: George G. Harrap and Co.
3. Russell MS. 2008 *The chemistry of fireworks*. London, UK: Royal Society of Chemistry.
4. Shimizu T. 1996 *Fireworks: the art, science, and technique*. Austin, TX: Pyrotechnica Publications.
5. Werrett S. 2010 *Fireworks: pyrotechnic arts and sciences in european history*. Chicago, IL: University of Chicago Press.
6. Kazuma S. 2004 *Hanabi no hon*. [*The book of fireworks*]. Kyoto, Japan: Tankosha.
7. Kazuma S. 2011 *Wonder of fireworks*. Tokyo, Japan: Soft Bank Creative.
8. Hoover WG, Hoover CG. 2009 Tensor temperature and shock-wave stability in a strong two-dimensional shock wave. *Phys. Rev. E Stat. Nonlinear Soft Matter Phys.* **80**, 011128/1–011128/6. (doi:10.1103/PhysRevE.80.011128)
9. Gregoire Y, Sturtzer M-O, Khasainov BA, Veyssiere B. 2009 Investigation of the behavior of solid particles dispersed by high explosive. In *40th Int. Annual Conf. of ICT, Karlsruhe, Germany, 23–26, June*. Munich, Germany: Fraunhofer.
10. Kudryashova OB, Vorozhtsov BI, Muravlev EV, Akhmadeev IR, Pavlenko AA, Titov SS. 2011 Physicomathematical modeling of explosive dispersion of liquid and powders, propellants. *Expl. Pyrotech.* **36**, 524–530. (doi:10.1002/prep.200900101)
11. Cabalo J, Schmidt J, Wendt JOL, Scheeline A. 2002 Spectrometric system for characterizing drop and powder trajectories and chemistry in reactive flows applied spectroscopy. *Appl. Spectr.* **56**, 1346–1353. (doi:10.1366/000370202760355073)
12. Martin-Alberca C, Garcia-Ruiz C. 2014 Analytical techniques for the analysis of consumer fireworks. *TrAC Trends Anal. Chem.* **56**, 27–36. (doi:10.1016/j.trac.2013.12.010)
13. Zohdi TI. 2004 A computational framework for agglomeration in thermo-chemically reacting granular flows. *Proc. R. Soc. Lond. A* **460**, 3421–3445. (doi:10.1098/rspa.2004.1277)
14. Zohdi TI. 2007 Computation of strongly coupled multifield interaction in particle-fluid systems. *Comput. Methods Appl. Mech. Eng.* **196**, 3927–3950. (doi:10.1016/j.cma.2006.10.040)
15. Zohdi TI. 2010 On the dynamics of charged electromagnetic particulate jets. *Arch. Comput. Methods Eng.* **17**, 109–135. (doi:10.1007/s11831-010-9044-3)
16. Zohdi TI. 2013 Numerical simulation of charged particulate cluster-droplet impact on electrified surfaces. *J. Comput. Phys.* **233**, 509–526. (doi:10.1016/j.jcp.2012.09.012)
17. Zohdi TI. 2014 Additive particle deposition and selective laser processing—a computational manufacturing framework. *Comput. Mech.* **54**, 171–191. (doi:10.1007/s00466-014-1012-6)

18. Zohdi TI. 2014 Mechanically-driven accumulation of microscale material at coupled solid-fluid interfaces in biological channels. *J. R. Soc. Interface* **11**, 20130922. (doi:10.1098/rsif.2013.0922)
19. Avci B, Wriggers P. 2012 A DEM-FEM coupling approach for the direct numerical simulation of 3D particulate flows. *J. Appl. Mech.* **79**, 010901-(1-7). (doi:10.1115/1.4005093)
20. Chow CY. 1980 *An introduction to computational fluid dynamics*. New York, NY: Wiley.
21. Schlichting H. 1979 *Boundary-layer theory*, 7th edn. New York, NY: McGraw-Hill.
22. Onate E, Idelsohn SR, Celigueta MA, Rossi R. 2008 Advances in the particle finite element method for the analysis of fluid-multibody interaction and bed erosion in free surface flows. *Comput. Methods Appl. Mech. Eng.* **197**, 1777–1800. (doi:10.1016/j.cma.2007.06.005)
23. Onate E, Celigueta MA, Idelsohn SR, Salazar F, Suárez B. 2011 Possibilities of the particle finite element method for fluid–soil–structure interaction problems. *Comput. Mech.* **48**, 307–318. (doi:10.1007/s00466-011-0617-2)
24. Leonardi A, Wittel FK, Mendoza M, Herrmann HJ. 2014 Coupled DEM-LBM method for the free-surface simulation of heterogeneous suspensions. *Comput. Part. Mech.* **1**, 3–13. (doi:10.1007/s40571-014-0001-z)
25. Onate E, Celigueta MA, Latorre S, Casas G, Rossi R, Rojek J. 2014 Lagrangian analysis of multiscale particulate flows with the particle finite element method. *Comput. Part. Mech.* **1**, 85–102. (doi:10.1007/s40571-014-0012-9)
26. Bolintineanu DS, Grest GS, Lechman JB, Pierce F, Plimpton SJ, Schunk PR. 2014 Particle dynamics modeling methods for colloid suspensions. *Comput. Part. Mech.* **1**, 321–356. (doi:10.1007/s40571-014-0007-6)
27. Zohdi TI. 2003 Genetic design of solids possessing a random-particulate microstructure. *Phil. Trans. R. Soc. Lond. A* **361**, 1021–1043. (doi:10.1098/rsta.2003.1179)
28. Zohdi TI. 2003 On the compaction of cohesive hyperelastic granules at finite strains. *Proc. R. Soc. Lond. A* **454**, 1395–1401. (doi:10.1098/rspa.2003.1117)